8.5

THE SENSITIVITY OF NUMERICALLY SIMULATED CYCLIC MESOCYCLOGENESIS TO VARIATIONS IN ENVIRONMENTAL PARAMETERS

Edwin J. Adlerman* and Kelvin K. Droegemeier
School of Meteorology and Center for Analysis and Prediction of Storms
University of Oklahoma, Norman, OK

1. INTRODUCTION

In a previous paper, Adlerman et al. (1999, AD99 hereafter), we used a three-dimensional numerical model to study the evolution of cylic mesocyclogenesis within a single supercell thunderstorm. Over a 4-hour period, the modeled mesocyclone underwent two distinct occlusions separated by an interval of approximately 3600 s. The overall behavior was consistent with conceptual models proposed by Lemon and Doswell (1979) and Burgess et al. (1982), and fit into the category of outflow-dominated or discrete cyclic regeneration proposed by Dowell and Bluestein (2000, 2002).

As a first step toward identifying and understanding the conditions necessary to produce cyclic redevelopments within supercell updrafts, Adlerman and Droegemeier (2002, AD02 hereafter) examined the effect of variations in model physical and computational parameters upon the cycling process. Changes in grid spacing, numerical diffusion, microphysics, and the coefficient of surface friction were found to alter the number and duration of simulated mesocyclone cycles. For example, a simulated supercell that underwent repeated mesocyclone cycling at a horizontal grid spacing of 1 km and smaller became a nearly steady-state unicellular storm when simulated at a grid spacing of 2 km. It was shown that the configuration of a numerical model could influence all of the important dynamics of cyclic regeneration to a degree that overwhelmed any intrinsic cyclic behavior.

With the additional understanding of the numerical model's influence upon cycling, we now seek to identify the environmental conditions necessary to produce cyclic redevelopment within a supercell updraft. This paper presents our preliminary findings.

2. METHODOLOGY

The simulation experiments are conducted using Version 5.0 of the Advanced Regional Prediction System (ARPS), a three-dimensional, compressible, nonhydrostatic model developed for storm scale numerical weather prediction (Xue et al. 2000, 2001).

Similar to AD99 and AD02, the numerical simulations are conducted using a horizontally homogeneous environment initialized with an ellipsoidal thermal bubble. The computational grid has uniform horizontal spacing of 0.5 km within a 100 x 100 x 16 km domain, with 43 levels in the vertical. The vertical grid spacing varies smoothly from 100 m at the ground to 700 m near the top of the domain. Fourth-order advection is used for both scalar and vector fields. Cloud microphysics is treated using the Kessler warm-rain parameterization scheme, while subgrid-scale turbulent mixing is represented using a 1.5-order turbulent kinetic-energy closure. The Coriolis force, surface friction, surface physics, and terrain are not included. The model is integrated for four hours, and history files are saved every five minutes.

3. SIMULATIONS

3.1 Control Simulation

In previous simulations by the authors (AD99; AD02), the horizontally homogeneous base state was initialized using a composited sounding associated with the well documented 20 May 1977 Del City, Oklahoma Storm (e.g. Ray et al. 1981, Johnson et al. 1987). In order to establish a control sounding that could be more easily manipulated, it was necessary to utilize an idealization of the Del City wind profile. After rotating the original Del City hodograph by 15 degrees, re-centering, and estimating its termination point at 10 km, the Del City hodograph can be

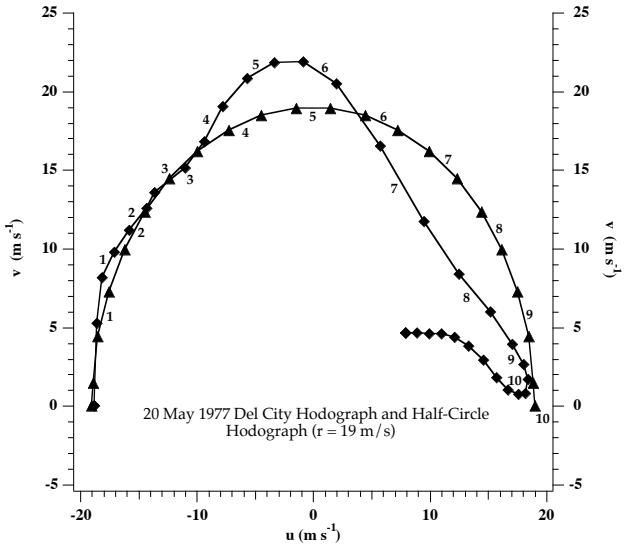

***Figure 1**: Plots of the original 20 May 1977 Del City hodograph and an idealized half-circle hodograph of radius 19 m s^{-1}. Approximate heights of points are indicated for altitudes of 1-10 km.*

*Corresponding author address: Edwin J. Adlerman, University of Oklahoma, CAPS/SOM, 100 E. Boyd. St., Rm 1310, Norman, OK 73019; email *eadlerman@ou.edu*

approximated by a half-circle hodograph of radius 19 m s^{-1} (Fig. 1), with uniform shear throughout the depth of turning (0-10 km). This yields a bulk Richardson number shear (BRNshear, 0-6 km) of approximately 13 m s^{-1}, compared to 12 m s^{-1} for the original Del City sounding.

When this idealized hodograph is used to initialize the model (the sounding remains the same), it produces a control simulation that is remarkably similar, though not perfectly identical to that reported in AD02. The principal storm develops into a mature supercell by 3600 s, with a pronounced hook echo and strong surface mesocyclone by 4200 s. The first occlusion cycle begins after 6600 s, with the development of a two-celled updraft structure and an occluded surface gust front. Surface vorticity peaks at 7200 s, and the first occlusion occurs shortly thereafter, with the development of a new surface mesocyclone by 7800 s.

The second occlusion cycle proceeds similarly to the first. Surface vorticity peaks in the occluding mesocyclone at 11400 s and the occlusion occurs at approximately 12000 s. A new mesocyclone develops once again to the east, and the storm continues without another occlusion through the remainder of the simulation (14400 s).

3.2 Variations in Shear Distribution

In order to explore the effects of changes in the distribution of shear, we systematically alter the location of points along the arc of the control case hodograph. Using a hyperbolic tangent vertical grid stretching function from the ARPS (Xue et al. 1995; AD02), we transform the uniform vertical distribution both downward and upward, which increases (decreases) upper (lower) level shear or decreases (increases) upper (lower) level shear. This method thus preserves the shape of the hodograph and the mean shear (6 x 10^{-3} s^{-1}), i.e. the length of the hodograph divided by the depth of turning (Rasmussen and Wilhelmson 1983).

Eight preliminary simulations were conducted, four in which the low-level shear was increased (simulations L1-L4, BRNshear 15-20 m s^{-1}) and four in which the upper-level shear was increased (simulations U1-U4, BRNshear 7-12 m s^{-1}). As the low-level shear is increased, the cycling process slows significantly for simulations L2 and L3, eventually ceasing entirely in the highest low-level shear simulation, L4. Compared to the control run, the first and second occlusion are delayed 2100 s for L2. In L3, the first occlusion is delayed by 4500 s, and no second cycle is observed.

For U1 through U4, no similar progression in the timing of the cycles is observed, possibly resulting from the smaller effect of upper-level shear upon low-level rotation. All four simulations cycle at least once, with the first occlusion always slower than in the control run. However, only U2 and U4 undergo two complete cycles. Despite the smaller low-level shears and resultant values of BRN that are greater than that of the standard supercell range (Weisman and Klemp 1982), all of the storms remain supercellular.

3.3 Variable Radii Simulations: 0-10 km Depth

In addition to the control run, four simulations were conducted using a half-circle hodograph with a turning depth of 10 km. Radii of 15, 25, 30, and 35 m s^{-1} were used (simulations $H_{10}1$-$H_{10}4$), covering a range of mean shears from 4.7 x 10^{-3} s^{-1} to 11 x 10^{-3} s^{-1} and BRNshears from 11-25 m s^{-1}.

The effects of the hodograph radii changes are quite varied, but do suggest that increasing shear throughout the same depth of turning tends to slow down and eventually stop the cycling process. $H_{10}1$ produces a small supercell that appears to be a miniature version of the control run. It produces two full cycles, with the first and second occlusions delayed by approximately 300 s. $H_{10}2$ produces a storm that appears very similar to the control run, except that it has a stronger surface mesocyclone and occludes only once at 9600 s.

$H_{10}3$ and $H_{10}4$ both produce supercell storms that are much larger in areal extent than in the control run and do not cycle throughout the entire simulation period. The differences in the sizes of the updraft and rainwater areas between the lowest and highest shear cases ($H_{10}1$ and $H_{10}4$) are quite striking (Fig. 2).

$H_{10}3$ and $H_{10}4$ exhibit quite different supercell structure toward the end of the simulation. $H_{10}4$ remains quite 'classic' throughout its lifetime. In contrast, $H_{10}3$ becomes less 'classic' and more 'high-precipitation' (HP) (Moller and Doswell 1988), with increasing amounts of rain wrapping around the upshear side of the mesocyclone. By 12300 s, its updraft and gust-front begin to stretch out into a

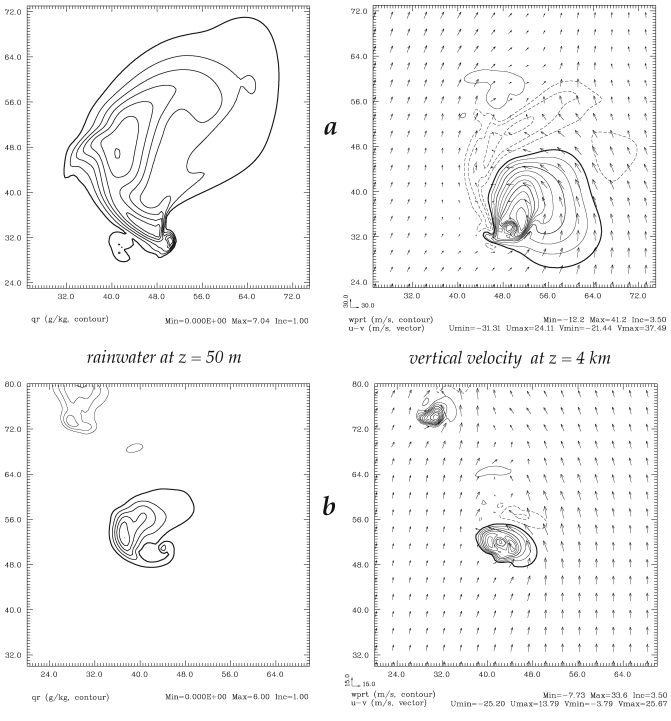

Figure 2: *Plots of rainwater mixing ratio at 50 m (left, contour interval 1 g kg^{-1}) and vertical velocity at 4 km (right, contour interval 3.5 m s^{-1}) at t = 11700 s, for (a) the $H_{10}4$ simulation and (b) the $H_{10}1$ simulation*

nearly north-south orientation and the storm appears to be transitioning toward a more outflow-dominated mode.

3.4 Variable Radii Simulations: 0-6 km Depth

In order to examine the effect of confining the turning layer to a smaller depth, five additional half-circle hodograph simulations were conducted, except with the turning depth confined to 6 km. The radii were chosen such that each simulation had the same corresponding mean shear as the previous half-circle runs, giving respective radii of 9, 11, 15, 18, and 21 m s^{-1} (simulations $H_6$1-$H_6$5) and BRNshears from approximately 9-21 m s^{-1}.

Similar to H_{10}1, $H_6$1 produces a very small supercell. However, it does not cycle throughout the duration of the simulation, and its surface mesocyclone remains relatively weak when compared to the control run.

Simulations $H_6$2 and $H_6$3 produce cyclic supercells that qualitatively resemble the control case but cycle more slowly. Compared to the control run, the first occlusions for $H_6$2 and $H_6$3 are delayed by 1200 s and 3000 s, respectively. The second occlusions are delayed by 2400 s and 2100 s, respectively.

Simulation $H_6$4 also produces a cyclic supercell, but similar to H_{10}3, it takes on a more HP character toward the end of the run. It undergoes its first occlusion at approximately the same time as the control run (7800 s), but its second occlusion is delayed to 14400 s, 2400 s later than the control.

In the highest shear simulation $H_6$5, the process of cyclic mesocyclogenesis occurs in an unusual mode that is not seen in any of the other curved-hodograph simulations. The first mesocyclone and associated hook echo (Figs. 3a-c) form as in the control run, with a strong vorticity maximum (A) extending from the surface upward through 4 km at 7800 s. However, since the surface winds behind the gust front remain mostly northerly (Figs. 3b,e) the surface mesocyclone does not occlude, but is pushed southward down the gust front. As the mid-level updraft also develops further southward (Fig. 3f), the mesocyclone center at 4 km remains well correlated with the surface mesocyclone. At the same time however, a new surface mesocyclone develops further *north* along the gust front with a new mid-level mesocyclone (B) also apparent (Figs. 3d-f). As this new mesocyclone moves further south (Figs. 3g-i), the old mid-level mesocyclone dissipates. The remaining surface vorticity is pushed southwestward and can be seen as a cyclonic flare in the rainwater contour (Figs. 3d,g). Throughout this transition the updraft never takes on a two-celled appearance (AD99), but remains unicellular, with the maxima shifting northward. This type of cyclic regeneration occurs again at 11100 s, after which the storm takes on HP characteristics.

3.5 Straight Hodograph Simulations

Five simulations were conducted using a straight hodograph, with the shear linearly distributed from 0-10 km. Similar to the half-circle runs, the length of the hodograph was chosen so as to keep the same range of mean shear as before. This results in hodograph lengths of 47, 59, 78, 94, and 110 m s^{-1} (simulations S1-S5), covering a range of BRNshears from 12-27 m s^{-1}.

Simulations S1 through S5 produce storms that are quite different than any of the previous curved-hodograph simulations. The storms tend to be less 'classic' in appearance, with smaller hook echoes and more linear areas of precipitation aligned nearly parallel to the gust front. Simulations S4 and S5 do not undergo cyclic mesocyclogenesis, and appear to be overwhelmed by the amount of shear. Only simulations S1, S2, and S3 show evidence of occlusion cycles. However, in all cases the occlusions are small-scale, and tend to be a mixture of the classic occlusion cycles of Burgess et al. (1982) and the patterns described in Figure 3. A more detailed examination of these simulations is required to understand the type of cyclic behavior exhibited.

3.6 Variations in CAPE

As a preliminary step toward investigating the role of CAPE in cyclic regeneration, we repeated the control case, with the base state thermodynamics replaced by the Weisman and Klemp (1982) analytic sounding. Low-level mixing ratios of 12-18 g kg^{-1} (simulations WK12-WK18) were used, covering a range of CAPE from 460-2963 J kg^{-1} (calculated using the virtual temperature correction and including water loading). This type of variation ignores the important influence of changes in the LCL and LFC of the sounding (e.g., Mc Caul and Cohen 2000).

As might be expected, these simulations were quite different than the control case. Soundings in which the CAPE was comparable to that of the Del City storm (i.e. mixing ratios > 15 g kg^{-1}) tended to produce storms that were more toward the HP end of the supercell spectrum than the control case, most likely a result of the higher water content in the analytic profile. In addition, the larger rain areas in these simulations initiated convection throughout the domain after 7200 s, which oftentimes interacted with the storm of interest and invalidated any further conclusions from the simulation. WK13-WK15 did exhibit some degree of regeneration, but none was as clearly cyclic as the control case, therefore making it difficult to conduct a study of CAPE variations. In order to obtain results that may be less ambiguous and more easily interpreted, a systematic variation of the Del City thermodynamics is necessary.

4. SUMMARY AND OUTLOOK

Several preliminary simulations were presented to examine how variations in the environment influence the process of cyclic mesocyclogenesis. Since this was the first attempt to investigate this issue, our parameter space was quite broad and could not yet be easily summarized or reduced. Although it was apparent that increasing the shear either throughout the troposphere or only near the ground often slows down cycling compared to the control case, there were several exceptions to this trend, including shifts in the mode of cyclic regeneration. In

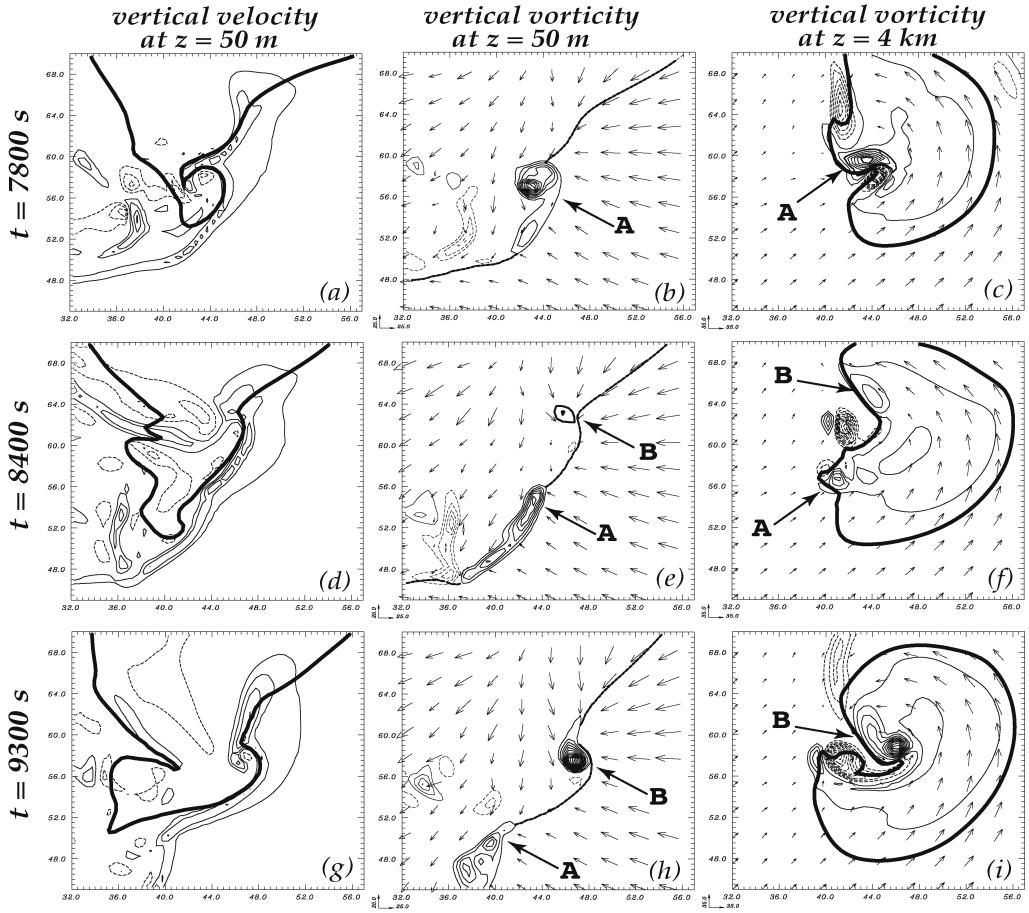

Figure 3: *Horizontal cross-sections of simulation H_o5 at t = 7800 s (a-c), 8400 s (d-f) and 9300 s (g-i). Left column: plots of vertical velocity at z = 50 m (contour interval 0.35 ms^{-1}); single dark contour is rainwater mixing ratio of 1 g kg^{-1}. Center column: plots of surface vorticity at z = 50 m (contour interval $5x10^{-3}$ s^{-1}); single dark contour is –1° C perturbation potential temperature contour. Right column: plots of vorticity at z = 4 km (contour interval $5x10^{-3}$ s^{-1}); single dark contour is updraft velocity of 5 m s^{-1}. A and B designate old and new mesocyclones, respectively.*

addition, soundings with identical CAPE and similar amounts of mean shear, BRNshear, and 0-3 km storm-relative environmental helicity produced supercell storms in which the timing and mode of cyclic mesocyclogenesis varied significantly. Further investigation is therefore needed to establish a more complete understanding of what physical processes correlate with changes in cyclic regeneration. In addition, a more comprehensive exploration of the parameter space is currently being undertaken and both will be reported in an upcoming paper.

ACKNOWLEDGEMENTS

The numerical simulations were performed on the National Science Foundation Terascale Computing System at the Pittsburgh Supercomputing Center. Support for this work was provided by the NSF through Grant ATM99-81130 to the second author and by Grant ATM91-20009 to the Center for Analysis and Prediction of Storms.

REFERENCES

Adlerman, E. J., K. K Droegemeier, and R.P. Davies Jones 1999: A numerical simulation of cyclic mesocyclogenesis, *J. Atmos. Sci*., **56**, 2045-2069.

Adlerman, E. J. and K. K. Droegemeier 2002: The sensitivity of numerically simulated cyclic mesocyclogenesis to variations in model physical and computational parameters, *in press for Mon. Wea. Rev.*

Burgess, D.W., V.T. Wood, and R.A. Brown, 1982: Mesocyclone evolution statistics. Preprints,*12th Conf. on Severe Local Storms*, Boston, MA, Amer. Meteor. Soc., 422-424.

Dowell, D.C., and H.B. Bluestein, 2000: Conceptual models of cyclic supercell tornadogenesis. Preprints, *20th Conf. on Severe Local Storms*, Orlando, FL, Amer. Meteor. Soc., 259-262.

Dowell, D.C., and H.B. Bluestein, 2002: The 8 June 1995 McLean, Texas Storm. Part II: Cyclic Tornado Formation, Maintenance, and Dissipation, *in press for Mon. Wea. Rev.*

Johnson, K.W., P.S. Ray, B.C. Johnson and R.P. Davies-Jones, 1987: Observations related to the rotational dynamics of the 20 May 1977 tornadic storms. *Mon. Wea. Rev.*, **115**, 2463-2478.

Lemon, L.R., and C.A. Doswell III, 1979: Severe thunderstorm evolution and mesocyclone structure as related to tornadogenesis. *Mon. Wea. Rev.*, **107**, 1184-1197.

Moller, A.R., and C.A. Doswell III, 1988: A proposed advanced storm spotter's training program. Preprints, *15th Conference on Severe Local Storms*, Baltimore, MD, Amer. Meteor. Soc., 173-177.

Mc Caul, E. W., Jr., and C. Cohen, 2000: The sensitivity of simulated storm structure and intensity to the lifted condensation level and the level of free convection. Preprints, *20th Conf. on Severe Local Storms*, Orlando, FL, Amer. Meteor. Soc., 595-598.

Rasmussen, E. N., and R. B.Wilhelmson, 1983: Relationships between storm characteristics and 1200 GMT hodographs, low-level shear, and stability. Preprints, *13th Conf. on Severe Local Storms*, Tulsa, OK, Amer. Meteor. Soc., J5-J8.

Ray, P.S., B.C. Johnson, K.W. Johnson, J.S. Bradberry, J.J. Stephens, K.K. Wagner, R.B. Wilhelmson, and J.B. Klemp, 1981: The morphology of several tornadic storms on 20 May 1977. *J. Atmos. Sci.*, **38**, 1643-1663.

Weisman, M. L., and J. B. Klemp, 1982: The dependence of numerically simulated convective storms on vertical wind shear and buoyancy. *Mon. Wea. Rev.*, **110**,504-520.

Xue, M., K. K. Droegemeier, and V. Wong, 2000: The Advanced Regional Prediction System (ARPS) - A multiscale nonhydrostatic atmospheric simulation and prediction tool. Part I: Model dynamics and verification. *Meteor. Atmos. Physics*., **75**, 161-193.

Xue, M., K. K. Droegemeier, V. Wong, A. Shapiro, K. Brewster, F. Carr, D. Weber, Y. Liu, and D. H. Wang, 2001: The Advanced Regional Prediction System (ARPS) – A multiscale nonhydrostatic atmospheric simulation and prediction tool. Part II: model physics and applications. *Meteor. Atmos. Physics*. **76**, 143-165.